



Spectral analysis of two Perseid meteors

J. Borovička¹ and H. Betlem²

¹Astronomical Institute, Ondřejov Observatory, 251 65 Ondřejov, Czech Republic

²Dutch Meteor Society, Lederkarper 4, NL-2312 NB Leiden, The Netherlands

Received for publication 28 January 1997

Abstract. Spectra of two bright (-11 mag) Perseid meteors are studied. Monochromatic light curves are constructed and the spectra are analyzed at selected points along the trajectory. The shift of maxima of low excitation iron lines down the trajectory in meteor flares is observed and explained by a longer radiative lifetime of the upper levels for these lines. Two spectral components with the temperatures of 4400–4800 K and 10,000 K, respectively, are identified in the spectra in accordance with previous findings. The ratio of both components, in terms of mass, varied smoothly from about 100:1 over 15:1 to 30:1. This ratio is not an unambiguous function of meteor velocity, height and brightness but depends on the previous evolution of ablation. The abundances of heavy elements are found consistent with the chemical composition of carbonaceous chondrites and the dust of comet Halley. Hydrogen, however, is not more abundant than in carbonaceous chondrites and thus significantly less than in cometary dust. The initial masses of the two meteoroids are estimated at 40 and 80 g, respectively. The meteor V-band luminous efficiency is found to vary in the range $\log \tau_v = -11.8$ to -12.0 in magnitude c.g.s. units. For the panchromatic luminous efficiency use of the value of -11.4 for bright Perseids is recommended. Nearly 1.5% of meteoroid kinetic energy is radiated out in the Ca II lines and 1% in all other lines between 3500 and 6600 Å. © 1997 Elsevier Science Ltd

from comet 109P/Swift–Tuttle and enter the Earth's atmosphere with a large velocity of 60 km s^{-1} . Very bright meteors are observed from time to time and if recorded with an objective grating photographic camera, their spectra can be studied in considerable detail.

Halliday (1961) published the most complete list of spectral lines identified in Perseid spectra. Using various photographic emulsions and cameras with dispersion from 50 to 120 Å mm^{-1} , he was able to identify 229 emission features in the region from 3680 to 8710 Å based on a combination of five meteor spectra. Later Halliday (1969) gave the line identifications down to 3100 Å based on one Lyrid and one Perseid spectrum. The ultraviolet lines in a Perseid spectrum were listed also by Harvey (1973a). Cook *et al.* (1971) performed photometric calibration of two Perseid spectrograms and were able to give line intensities in absolute units. In addition to these photographic works, which dealt with very bright meteors of magnitudes around -10 , spectra of fainter Perseids (magnitudes around 0) were observed with lower dispersion using television techniques (Millman *et al.*, 1971; Borovička and Boček, 1995).

All photographic observations gave the same general picture of a bright Perseid spectrum: the H and K lines of ionized calcium at 3934 and 3968 Å are the brightest lines. Other bright lines include ionized magnesium at 4481 Å, neutral magnesium triplet at 5167–5184 Å, neutral sodium doublet at 5890–5896 Å and neutral oxygen triplet at 7772–7775 Å. Numerous lines of neutral iron are also present. Other atoms and ions reliably identified are H I, N I, N II, Al I, Si II, Ca I, Cr I, Mn I, Fe II, Ni I, and Sr II. The identification of O II, Si I, Sr I, Ba I, and Ba II in Perseid spectra remained doubtful. On the other hand, the presence of the first positive bands of the nitrogen molecule has been well established.

An indication that the Ca II lines are fainter relative to O I in fainter meteors was noted (Millman and Halliday, 1961). In faint TV spectra the Ca II lines are no more dominant (if present at all) and the brightest are the lines of O I and Mg I. In bright meteors it was noted that the brightness of the Ca II lines relative to O I increased along

Introduction

The Perseid meteor shower is a major shower for northern hemisphere observers with a reliable display peaking around August 12 each year. This makes the Perseids one of the most common targets of meteor observations (including spectroscopy). The meteoroids are derived

the trajectory and that Ca II is especially strong in terminal flares (Millman and Halliday, 1961; Halliday, 1961). Cook *et al.* (1971) mentioned that also the H I and Si II lines increase in strength relative to the rest of the spectrum down the meteoroid trajectory. Borovička and Boček (1995) observed a Perseid flare with a TV camera. All meteoric emissions increased in the flare much more dramatically than the emissions of atmospheric origin due to O I and N I. Another effect in a Perseid flare was observed by Russel (1960): The low excitation lines of neutral iron had their maxima shifted to lower heights with respect to other lines.

In general Perseid spectra are similar to the spectra of other fast meteors. For example the Orionids (67 km s^{-1}) show the same lines and spectral development along the trajectory as the Perseids (Halliday, 1987). Since there are more good quality spectra available for Perseids than for any other shower, Perseid spectra can be used to study the formation of the fast meteor spectra and can serve as clues for their interpretation. Possible minor differences in spectra could then reveal possible chemical or structural differences among meteoroids of different showers or within one shower.

Quantitative analyses of Perseid spectra are, however, much rarer in the literature than qualitative descriptions. Harvey (1973a) assumed Boltzmann distribution of level populations and optically thin radiation in his analysis. He computed the effective radiation temperature from the intensity ratios in pairs of lines. The temperature near 3000 K was derived for Fe I lines in one Perseid spectrum but quite different temperatures were found for three other atoms. The elemental abundances corrected for partial ionization and dissociation were later given in Harvey (1973b). However, the assumption of optical thinness is inadequate for meteors as bright as magnitude -9 (Borovička, 1993) and the simple method used by Harvey cannot be considered as yielding reliable results.

Only few lines were measurable in the Perseid spectra analyzed by Kokchirova (1993). She modified the method of Harvey (1973a) by using the intensity ratios of lines of different elements and assuming the chemical composition. However, the ionization of elements like sodium was not taken into account and the obtained excitation temperatures in the wide range of 1500–12,000 K have, in our opinion, no physical meaning.

A new method of meteor spectra analysis was developed by Borovička (1993) in connection with the study of a slow fireball. A synthetic spectrum was computed and the free parameters—excitation temperature, column densities of various atoms, and effective cross-section of the radiating volume—were adjusted by the least squares method. Following Ceplecha's method (Ceplecha, 1964) of emission curve of growth, self-absorption was fully taken into account and the Boltzmann population of levels was assumed. It was found that the spectrum can be well explained by assuming two components of quite different temperature.

The two spectral components were studied in more detail by Borovička (1994) in four bright meteors of different velocities. The two spectral components were present in all four meteors with nearly the same temperatures, 4000–4500 K for the so-called main spectrum and about 10,000 K for the so-called second spectrum.

Table 1. Atmospheric trajectory of two Perseid fireballs

Meteor No.	DMS-85016	DMS-89046
Date	1985 Aug. 12	1989 Aug. 13
Time UT	2 h 11 min 20 s	2 h 27 min 40 s
h_B (km)	117.5	108.1
h_E (km)	70.3	72.6
v_∞ (km s^{-1})	60.6 ± 0.4	60.9 ± 0.5
v_E (km s^{-1})	57 ± 2	58 ± 2
z_R	$28^\circ 8'$	$27^\circ 0'$
L (km)	53.6	39.8
D (s)	0.90	0.66

Explanation of symbols: h_B , beginning height; h_E , terminal height; v_∞ , initial velocity; v_E , terminal velocity; z_R , zenith distance of the radiant; L , total trajectory length; D , total duration.

The main spectrum contains lines of neutral atoms, especially Na, Mg, Fe, Ca, Cr, Mn, Al and ionized Ca. In the second spectrum most metals are ionized and the main contributing lines are those of ionized Ca, Mg, Si, Fe and neutral O, N, H (which have high ionization potential). The main result was that the ratio of the mass of the gas involved in the production of the main and the second spectrum, respectively, m_1/m_2 , is a strong function of velocity. It was about 3000 in the slow 17 km s^{-1} fireball but decreased to 15 in a 67 km s^{-1} Orionid. Different strength of the second component is the main factor which discriminates the spectra of slow and fast fireballs. It is probable that the second component is related to the shock wave formed in front of the meteoroid.

The analysis in Borovička (1994) was restricted to the brightest points of four fireballs. The aim of this paper is to study the development of both spectral components along the trajectory. For this purpose two spectra of bright Perseids photographed in the Netherlands were analyzed. This is the first quantitative analysis of Perseid spectra which recognizes the two components and takes the self-absorption fully into account. The analyzed spectra are also used to derive chemical composition of Perseid meteoroids and to study the luminous efficiency of fast meteors.

Observational material

The meteors analyzed here are DMS-85016 (Dutch Meteor Society meteor No. 16 in 1985) of August 12, 1985 and DMS-89046 of August 13, 1989. Both were photographed by a network of directly imaging cameras equipped with rotating shutters which enabled the trajectory, velocity and orbit to be fully determined. The meteors have been described in more detail in Betlem and de Lignie (1985) and van Oudheusden and van Dijk (1991), respectively. A summary of the data on their atmospheric trajectories is given in Table 1. An absolute photographic magnitude of about -11 was reached in both cases. The photometry and associated problems are, however, discussed below in connection with the luminous efficiency.

The spectra were obtained at station Bussloo, in the Netherlands with a $f = 16 \text{ cm}$ Zeiss Tessat camera and a $400 \text{ grooves mm}^{-1}$ grating using Kodak Tri-X sheet film. No shutter was present. The spectrum of DMS-85016 (here-

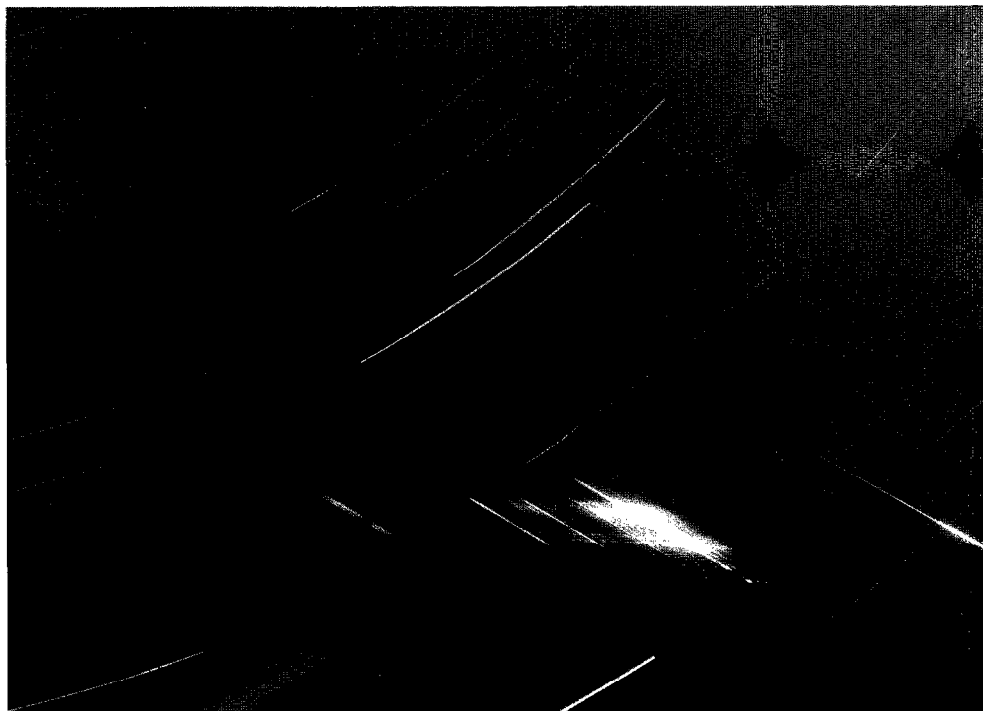


Fig. 1. The spectrum of meteor DMS-85016 (spectrum A). The meteor flew from top left to bottom right. Part of the zero order image is visible on the right. The bright lines near the blue end of the spectrum are visible also in the second order

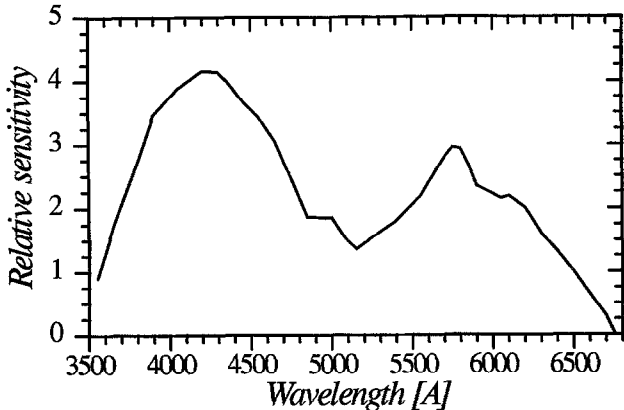


Fig. 2. Relative sensitivity of our spectrograph as a function of wavelength. Normalized at 6500 Å

after referred to as spectrum A) is reproduced in Fig. 1. The transmissivity of the optics and the sensitivity of the photographic material enabled the wavelengths from 3500 to 6600 Å to be covered. The spectral sensitivity of the system was determined by measuring the spectrum of α Lyrae recorded in the same frame as spectrum A and dividing it by the known energy distribution in the A0 V star spectrum (Sviderskiene, 1988). The sensitivity function for the first spectral order is given in Fig. 2. As the distances of the meteors from the camera (nearly 185 km for the bright parts of both meteors) and the meteor angular velocities (18° s^{-1}) were known, the absolute calibration of the spectra was possible. Owing to the angle of only about 30° between the meteor direction and the dispersion line, the effective dispersion was approximately 300 Å mm^{-1} in both cases.

The light curves of both meteors are similar. For a long time the meteors are relatively faint and the brightness increases slowly. Then the brightness rises abruptly and a period of intensive radiation follows. Toward the end the meteors become fainter with several distinctive flares of moderate brightness. A sufficient number of lines in the spectra is available only during the period of intensive radiation and the detailed analysis will therefore be restricted to this part of the trajectory.

Line identifications and monochromatic light curves

Both spectra are remarkably similar and are quite typical for Perseid meteors. The H and K lines are by far the most intense features along the whole trajectory. At the beginning, they are the only visible lines. The infrared oxygen lines, which could be of comparable brightness at the beginning, lie outside our spectral range. The other bright lines present in the visual region are also well known from the spectra of Perseids and other fast meteors.

The identification of the main spectral features is given here in Fig. 3 where the two spectral components, computed by the method of Borovička (1993), are also shown. The tracing of spectrum A in the flare at the height of 79.5 km is given in the upper part of the figure. The computed synthetic spectra of the main component (temperature $T = 4800 \text{ K}$, column density of neutral iron $N_{\text{FeI}} = 1.5 \times 10^{15} \text{ cm}^{-2}$) and the second component

($T = 10,000 \text{ K}$, $N_{\text{FeII}} = 10^{14} \text{ cm}^{-2}$) are given below it. The lines are identified by the name of atom/ion. For a more detailed identification see the list of observed lines in Hallday (1961) or of computed lines in Borovička (1994). The Ca II lines are produced mostly in the second spectrum although they are predicted to be present also in the main component.

In addition to the species mentioned in Fig. 3, also Cr II (multiplet 44) and Ti II (82) may contribute to the lines observed at 4550 and 4585 Å, together with Fe II (38) which is the main contributor. The $H\beta$ line at 4861 Å may be present as a faint feature near the Fe I line. Cr II, Ti II and H I all belong to the second spectrum.

Two methods were used to study the temporal evolution of the spectral components. Firstly, several lines were measured along the trajectory and monochromatic light curves as a function of height were obtained. Secondly, the spectrum was completely analyzed at selected points along the trajectory and the mass ratio of both components of gas was determined. Both approaches were restricted to the bright parts of the meteor trajectory.

Representative monochromatic light curves are given in Fig. 4. The main spectrum is represented by the sodium doublet. Other lines of the main component behaved similarly except for the low multiplets of iron (see below). In spectrum A a broad maximum occurred between 85 and 82 km and two shorter flares are present at 79.5 and 78.5 km. In spectrum B the former maximum is missing completely, two bright flares are present at 79 and 78 km and one fainter at 77 km.

The lines of iron multiplets 1 and 2 show the effect described by Russel (1960); the flares are shifted down the trajectory relative to the other lines. This is clearly visible by a visual inspection of original negatives and also in Fig. 4 where the light curve of one Fe I (2) line is presented. The multiplets 1 and 2 are low excitation intercombination lines originating from metastable levels and are, as noted already by Russel (1960), typical for the radiation of the meteor wake. Other intercombination lines, e.g. Mg I multiplet 1, would probably show the same effect, if they were clearly visible in the spectrum.

The explanation of the strength of intercombination lines in the wake and the shift of their flares lies probably in slower de-excitation of metastable levels after the atoms leave the hot radiating volume. We present here a possible qualitative explanation of the Russel effect. The situation in a flare is demonstrated schematically in Fig. 5. The physical processes involved are shown in the upper part of the figure. The time history of an individual atom can be read by drawing a horizontal line. The flare starts as a result of subsequent evaporation of a large amount of material in a short time interval. After evaporation, the atoms reach a hot region of gas in nearly thermal equilibrium (TE) with Boltzmann population of levels maintained by mutual collisions of atoms, ions and free electrons. This region is the main source of the main spectrum radiation. After a time (sometimes called the *relaxation time*) atoms leave the hot region and reach a region where the collisional frequency decreases. There is no mechanism to maintain stable populations of excited levels and atoms de-excite, primarily by radiative transitions. The low-lying metastable levels, however, de-excite more slowly because of smaller transition probability from them. Nevertheless,

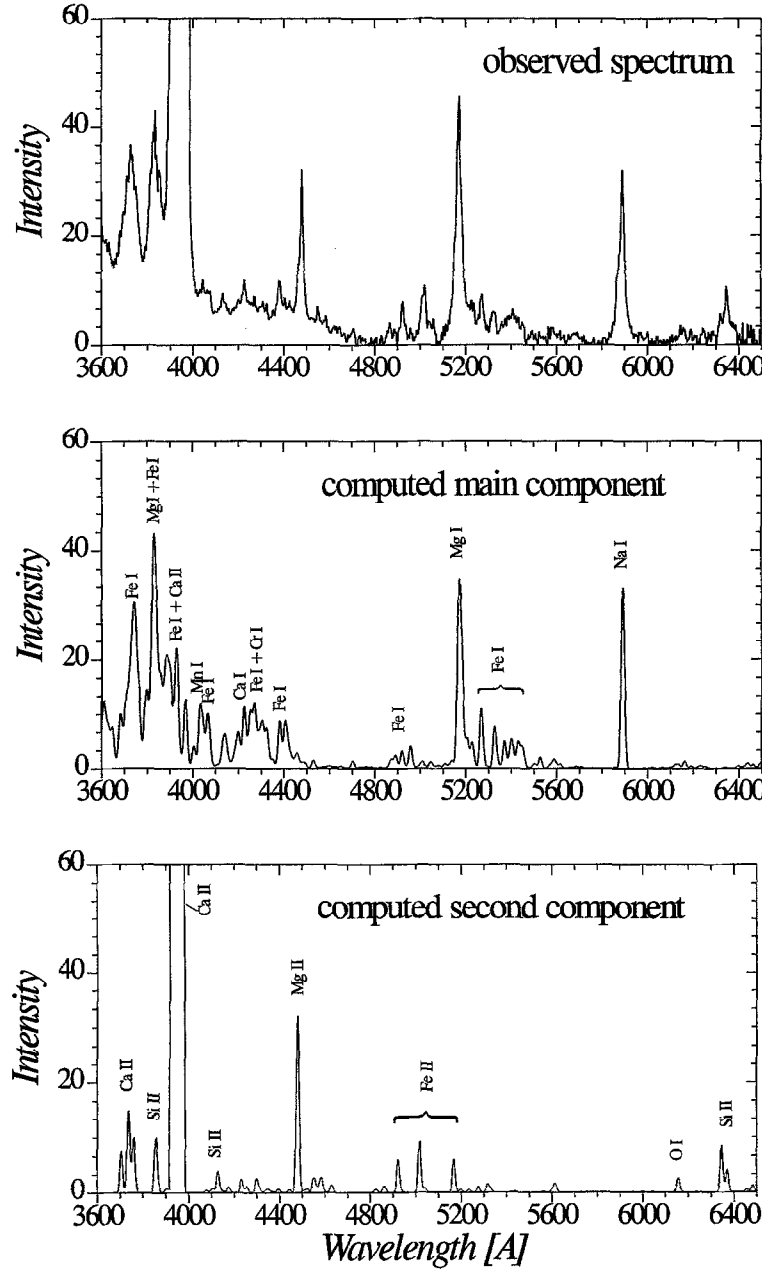


Fig. 3. The calibrated photometric tracing of spectrum A at the height of 79.7 km (above) and the computed synthetic spectra of the main and second spectral components. The observed spectrum is slightly out of focus above 5500 Å. The intensity scale is in units of $10^9 \text{ erg s}^{-1} \text{Å}^{-1} \text{sr}^{-1}$ while the instrumental width of individual lines is about 10 Å. The Ca II lines are out of the given scale, their computed intensities in the second spectrum are 750 and 500. The observed intensities are about these values or more, the calibration is uncertain due to overexposure

the effective lifetime must not be exactly the radiative lifetime of the levels because some collisional excitation from the ground state can still occur. Moreover, the level population is also enhanced by downward transitions from higher levels.

In the lower part of Fig. 5, the number of allowed and intercombination radiative transitions in the whole meteor is shown as a function of time. For an optically thin line this number is directly proportional to the line intensity. For an optically thick line the situation is more complicated and depends on geometry but the overall picture will be the same. Before the flare, the allowed

and intercombination lines are at their (different) quiet intensities. In the flare, the number of allowed transitions is proportional to the number of atoms in the TE region. Similarly, the number of intercombination transitions is proportional to the population of metastable levels. At the final de-excitation of the highly excited levels, the population of the metastable levels is enhanced above its equilibrium value by downward cascade transitions from the high levels. These downward transitions are, of course, present also before but they are not important in the TE region because the level populations are maintained here by much more frequent collisional transitions.

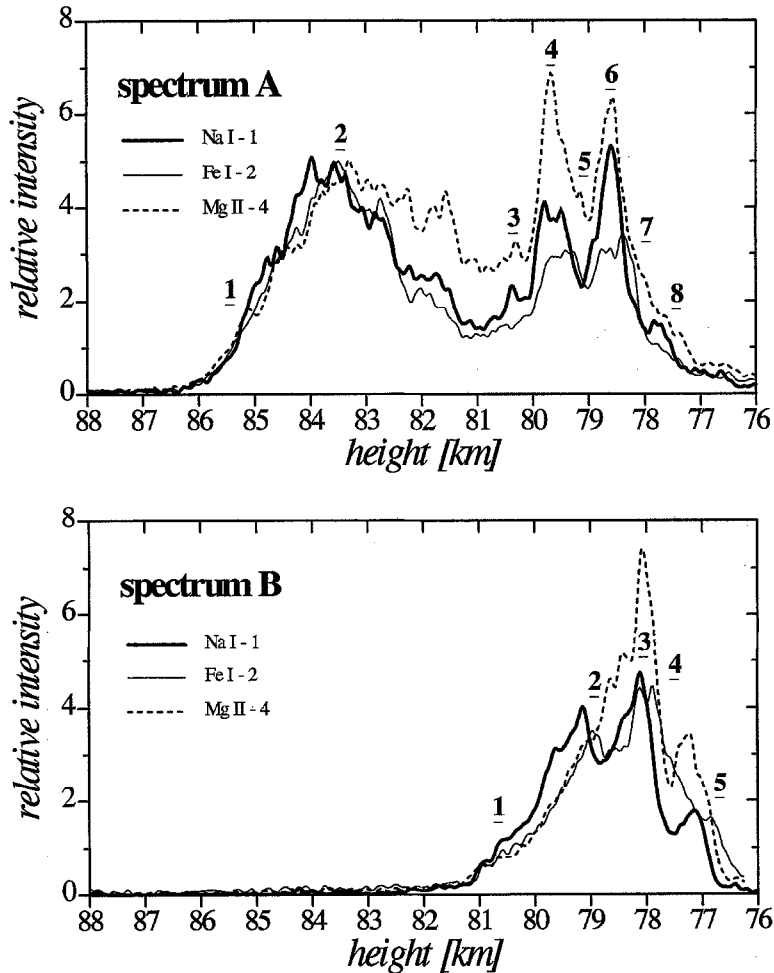


Fig. 4. Monochromatic light curves in three representative spectral lines: the unresolved sodium doublet (5890 and 5896 Å), the Fe I multiplet 2 line (4427 Å), and the Mg II line (4481 Å). The curves have been normalized to reach the same intensity around 84 km of height in spectrum A and around 79 km in spectrum B. The underlined numbers designate the points where the spectrum has been analyzed (see Table 2)

The final relation of the two lines in Fig. 5 is similar to what is observed, especially in the flare at 79.5 km in spectrum A (Fig. 4). Things are certainly more complex in reality than shown here, but it has been demonstrated at least that the temporal shift of the intercombination lines is understandable. There is no reason to consider the intercombination lines as a distinctive spectral component, they are excited in the same region as the other lines of the main component.

The second component is represented in Fig. 4 by the line of the ionized magnesium. It is clearly seen that the Mg II line, in comparison with Na I, is relatively faint at the beginning and bright toward the end. Of particular interest is the comparison of spectra A and B below the height of 80 km, where two flares of Na I are present in both cases. While the Mg II line is faint during the first flare in spectrum B, in spectrum A (where one bright maximum already occurred at about 84 km) Mg II is bright in both flares. This demonstrates that the intensity ratio of both lines is not an unambiguous function of meteor height, brightness etc. but depends on the history of the meteor. The lines of Si II and Fe II show the same behavior as Mg II. For Ca II this behavior seems to be less pronounced but the calibration of the very bright lines

represents some problem. The relation of the two spectral components was further studied by the analysis of the spectra at selected points.

Physical analysis of the spectra

The spectra were analyzed by the method of Borovička (1993) at the points marked in Fig. 4. The resolution of the spectra did not allow quite unambiguous solutions. In particular, the column density and cross-section could not be clearly separated. However, their product, which gives the total number of atoms in the radiating gas, could be obtained with confidence. The effective excitation temperature of the main component gas was determined with the estimated precision of ± 200 K. For the second component the temperature of 10,000 K was found quite satisfactory and was used as fixed for all points. The resulting temperature, T , of the main component, total number of neutral iron atoms, N_{FeI} , in the main component, and iron ions, N_{FeII} , in the second component gas are given in Table 2.

The temperature of the main component was found

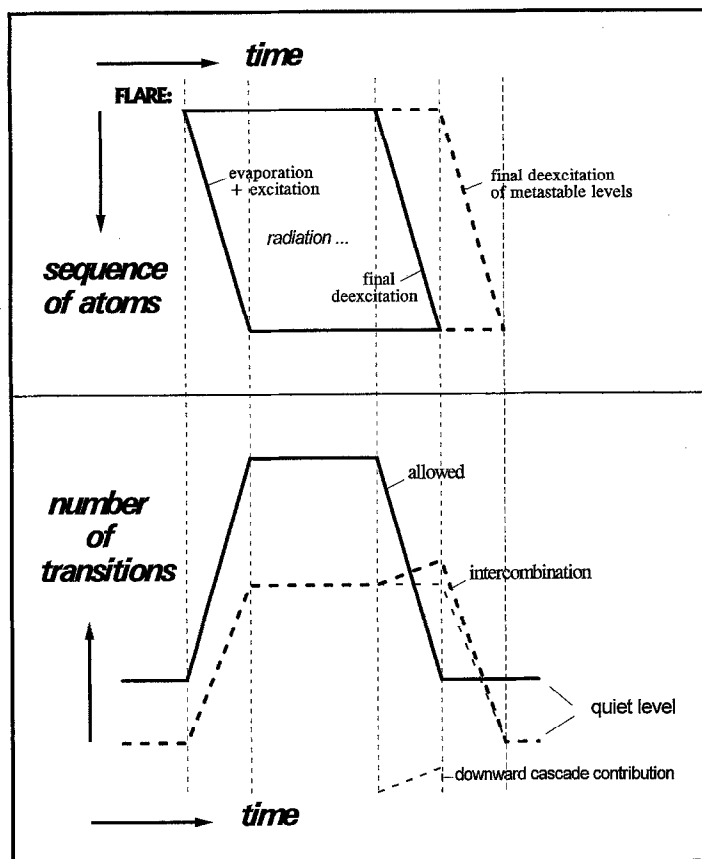


Fig. 5. Schematic representation of a meteor flare and the explanation of the shift of maxima of intercombination lines. See the text for more explanation

Table 2. Two spectral components in Perseid spectra

Point No.	Height (km)	Main component			Second component $N_{\text{FeII}} = N_{\text{Fe}}$ ($\times 10^{19}$)	Ratio m_1/m_2
		T (K)	N_{FeI} ($\times 10^{19}$)	N_{Fe} ($\times 10^{19}$)		
<i>Spectrum A</i>						
1	85.2	4650	530	1300	18	70
2	83.6	4600	1300	2500	35	70
3	80.3	4800	200	500	30	16
4	79.7	4800	390	800	60	13
5	79.1	4650	400	800	40	20
6	78.6	4700	850	1700	60	28
7	78.0	4750	350	800	30	28
8	77.5	4450	380	600	17	35
<i>Spectrum B</i>						
1	80.5	4350	540	900	9	100
2	79.0	4550	600	1200	30	40
3	78.1	4750	450	1100	55	20
4	77.4	4550	260	550	20	27
5	76.7	4850	140	500	15	33
<i>Meteor No. 221 (Cook et al., 1971)</i>						
6.2	87.9	4600	750	2100	100	21
7.2	83.8	4600	600	1700	70	24
<i>Meteor No. 233 (Cook et al., 1971)</i>						
6.1	81.8	4600	500	1500	60	25

typically between 4500 and 4800 K. This is in the upper part of the range derived in previous meteor analyses with the same method (Borovička, 1993, 1994; Borovička and Spurný, 1996). The fact that temperatures of both spectral components do not depend on meteor velocity was confirmed again.

To obtain the ratio of the mass of ablation products involved in the production of both components, we can use the ratio of the number of iron atoms as the mass percentage of iron is assumed to be the same in both components and equal to the iron mass percentage in the meteoroid. However, only neutral iron is observed in the main spectrum and only ionized iron is observed in the second spectrum. We have therefore to estimate the ionization degree of iron to obtain the total iron content. The ionization degree depends on temperature and the density of free electrons. The temperature is known, the electron density can be computed by the method described in Borovička (1993) under some assumptions as to the geometry of the radiating volume and provided that the abundances of the elements contributing most of the free electrons are known.

For the second spectrum it was found that almost all iron is singly ionized for a relatively wide range of parameters around the most probable iron density of 10^{14} cm^{-3} (Borovička, 1994). The derived amount of Fe II is therefore equal to the total amount of iron. The situation is more complicated for the main spectrum. The most probable combinations of column density and cross-section were used to estimate the size and density of the radiating volume. The main contributors of free electrons proved to be magnesium, iron, and to some extent silicon. Silicon is not observable directly in the main spectrum but its contribution could be estimated from the supposed chemical composition. The following range of parameters was then found at various points in the two meteors: diameter of the radiating column, 8–16 m, and electron density from 3×10^{12} to $2 \times 10^{13} \text{ cm}^{-3}$. It followed that 40–60% of iron was ionized. The total amount of iron in the main component gas at various points is also given in Table 2. Finally, the ratio of iron content in the main component to the second component is given in the last column.

The ratio is changing in the way already seen in monochromatic light curves. The share of the second component is low at the beginning of the bright part of both meteors, with $m_1/m_2 \approx 70\text{--}100$. Then the relative importance of the second component grows and the ratio decreases to 15–20. Toward the end the ratio exceeds 30 again. It should be noted that the high share of the second component is not correlated with meteor flares. This can be seen well in spectrum A. The second component is strong not only in the flare at 79.5 km but also before this flare. On the contrary, it is two times weaker in relative scale in the subsequent flare at 78.5 km. The ratio of both components changes more slowly than the amount of mass in both components themselves.

To be able to compare the present results with other meteors, two meteors analyzed by Cook *et al.* (1971) have been evaluated by our procedure, using the absolute intensities of important lines given by the authors. Because of a more limited amount of data available, the reduction was more uncertain. Nevertheless, some estimates have

been obtained and are given in Table 2. The items dependent on the ionization correction are most uncertain and are printed in italics. The column density seemed to be lower in these meteors, yielding larger radiating volume, lower density and higher ionization. This may be a consequence of larger height where these meteors reached their maximum brightness. Nevertheless, the final ratios m_1/m_2 are very similar to those in our meteors.

The mass ratio of both components as a function of meteor velocity was studied by Borovička (1994). Each meteor was, however, analyzed only at its brightest point. The lowest ratio was found in a 67 km s^{-1} Orionid: $m_1/m_2 = 15$. The Perseids analyzed here reach comparable values in the middle of their bright part. The ratio, however, changes along the trajectory and the share of the second component is much lower at the beginning. This is the reason for the increase of the brightness of some lines relative to other lines as mentioned by several authors (Cook *et al.*, 1971; Millman and Halliday, 1961).

The observations of other authors show that the lines of the second component are fainter in faint Perseids which radiate at higher height (e.g. Millman *et al.*, 1971). Nevertheless, as mentioned already in the previous section, no function relating directly the ratio of both components with meteor brightness or height (for a given velocity) can be given. In fact, the share of the second spectrum rises with some delay after the ablation rate has increased dramatically. This can be tentatively interpreted as a consequence of development of a strong ablation shock wave. Some modelling would, however, be needed to explain the origin of the second spectral component definitely. Note that Borovička and Boček (1995) observed the line of Na I to brighten *after* Ca II and Mg II, which is in contradiction with the present observations. However, this could be caused by a low time resolution of 0.04 s. A similar effect would appear for example, if we compared the points 4 and 6 of spectrum A (Fig. 4). They are 0.02 s apart.

Another interesting question is the behavior of oxygen and nitrogen lines. We observe only one faint oxygen line in our spectra, which is insufficient for detailed analysis. However, the infrared O I and N I lines are common in Perseid spectra. They appear early, do not brighten along the trajectory in such a way as Ca II lines and other lines of the second component, show much smaller amplitude in flares, and are strong also in faint Perseids (Borovička and Boček, 1995; Halliday, 1961; Millman and Halliday, 1961). These lines are certainly of atmospheric and not meteoritic origin. They need high temperature for excitation and are in fact fully consistent with being excited in the same region as the second spectrum under the temperature of 10,000 K. The same is valid also for the N₂ molecule. We can therefore interpret the situation so that the 10,000 K region is always present in Perseids and other fast meteors and the relative amount of meteoritic to atmospheric material in it is variable. A large amount of meteoritic material is present only during the high ablation phase in bright meteors. But if we identify the second spectrum region with the shock wave, the question arises, whether the shock wave can be present also at large heights and in faint meteors. These questions are to be studied in the future. It is highly probable that atmospheric material is present in large amounts also in the

main spectrum region but does not radiate at lower temperatures. Note also that the N II lines observed by Halliday (1961) correspond to a temperature of the order of 30,000 K. These lines are probably not excited by thermal processes.

Chemical composition

Since we were able to estimate the ionization degree in the radiating gas, we can infer the abundances of the observable elements. In addition to Fe I, the column densities of Na I, Mg I, Ca I, Cr I and Mn I in the main component could be estimated from the spectra. These column densities are, however, based on only one or a few lines, and in all cases except Na I the lines were blended with iron lines. It is therefore not surprising that abundances determined at various points showed very large scatter reaching a factor of four between individually determined values. We have therefore computed average relative abundances at points 2–7 in spectrum A and at points 1–5 in spectrum B.

Also the second component could be used to derive ratios of some elements. A temperature of 10,000 K was assumed. Since all lines, except Ca II H and K, are optically thin, the relative abundances are not dependent on the assumed column densities. The Ca II abundance was not determined because H and K lines are too bright for analysis and the lines of multiplet 3 could not be separated from lines of the main component.

The results for both components are given in Table 3 together with the average abundances in carbonaceous chondrites of type C1, which are the meteorites with chemical composition most close to the original composition of solar system material (Anders and Grevesse, 1989). The abundances in the dust of comet Halley as obtained from *in situ* mass spectroscopy (Jessberger *et al.*, 1988) is also given for comparison because Perseids are cometary meteors. Iron is used as reference element because it has by far the most numerous lines in meteor spectra and the ratios to iron are the most reliable ratios obtainable from meteor spectroscopy.

Most values in Table 3 are within a factor two of the chondritic and cometary values, which is inside of the expected error. In fact, this consistent result is very satisfying because of the above described difficulties and the fact that the ionization correction was extremely large for some elements. It was computed that 99.5–99.8% of sodium and 98.5–99.3% of calcium was ionized at various points along the meteor trajectories. In summary, it seems

that Perseids have quite normal chemical composition, at least for the observable elements. Possible minor deviations are discussed below.

The good agreement of calcium abundance with meteoritic value is remarkable. In many meteors, calcium is depleted in the radiating gas owing to incomplete evaporation (Borovička, 1993; Borovička and Spurný, 1996). A good example is the Benešov bolide, a stony body of the estimated initial diameter of 2 m and velocity of 21 km s⁻¹ (Borovička and Spurný, 1996). The abundance of calcium in the radiating gas was more than two orders of magnitude lower than in chondrites at the height of 78 km, i.e. a height similar to that of the present meteors. The Benešov bolide, however, reached much lower heights and the calcium abundance was found normal at 25 km. Here, the spectrum was quite unusual owing to the prominent role of Ca I lines. On the contrary, Perseid spectra do not show unusually bright Ca I lines because most calcium is ionized owing to the low density of the gas. The complete evaporation, reached in the Benešov bolide only in dense atmospheric layers, was achieved in Perseids high in the atmosphere, obviously because of their high velocity and a more violent ablation. The temperature of the main component gas was by about 1000 K higher in Perseid meteors than in the Benešov bolide at similar heights.

A high Si/Fe ratio was found in comet Halley and the Mg/Fe ratio was also relatively high. The Si abundance as determined from the Perseid second spectral component is also higher than in chondrites, although lower than in Halley. For Mg the situation is unclear. This is the only element with abundances determined independently from both spectral components. The values differ by a factor of two. The abundance in main component may be slightly overestimated owing to the blend of the bright Mg I line with lines of Fe I and Fe II. On the other hand, the abundance derived from the second component depends on the assumed temperature. If the temperature were lower than 10,000 K, the abundances of both Mg and Si must have been higher. We conclude that a factor of two lies within the observational errors and that the Mg and Si abundances are consistent with chondritic values.

Volatile elements are of particular interest. As N and O come from the Earth's atmosphere, only hydrogen is evidence of the volatile content of Perseid meteoroids. In contrast to the spectra of Cook *et al.* (1971), our spectra do not show the H α line at 6563 Å. It lies near the sensitivity limit of the film and the spectrum is not particularly well focused in this region but, nevertheless, the line should be visible. From its absence we can obtain an upper limit to the hydrogen abundance (see Table 3). The faint

Table 3. Relative elemental abundances by number in two Perseid spectra, C1 chondrites and comet Halley dust

		Fe	Na	Mg	Si	Ca	Cr	Mn	H	N	O
spec. A	main component	1	0.10	2.2		0.06	0.010	0.014			
	2nd component	1		1.0	2.5				2	< 50	30
spec. B	main component	1	0.09	2.0		0.05	0.005	0.013			
	2nd component	1		1.1	2.0				3	< 50	30
C1 chondrites ^a		1	0.06	1.2	1.1	0.07	0.015	0.011	6	0.07	9
1P/Halley dust ^b		1	0.19	1.9	3.5	0.12	0.017	0.010	40	0.8	17

^a Anders and Grevesse (1989).

^b Jessberger *et al.* (1988) as cited in Anders and Grevesse (1989).

$H\beta$ line is nearly consistent with this limiting value, which may therefore represent the real H abundance. It is lower than in carbonaceous chondrites. Analyzing the spectra of Cook *et al.* (1971), we found values of $H/Fe = 4-6$, consistent with chondritic value. Using the $H\beta$ line in the TVS 29 spectrum of Borovička and Boček (1995), we found $H/Fe \approx 5$. It can therefore be concluded that the Perseid spectra analyzed so far show hydrogen abundance comparable or lower than in carbonaceous chondrites and significantly lower than in comet Halley dust. This can be easily explained by considering that meteoroids released from the parent comet lose their volatiles when they are orbiting the Sun.

The upper limit of the nitrogen abundance in the second component gas, derived from the absence of N I lines near 5610 \AA , is relatively low when compared with oxygen. The ratio $N/O \leq 1.5$ is obtained which can be compared with $N/O \approx 4$ in the Earth's atmosphere. One possible explanation could be that a substantial part of the oxygen in the spectrum is of meteoritic origin. This would, however, need $O/Fe > 18$ in the meteoroid which seems improbable considering the low content of hydrogen. Another explanation is that due to the high dissociation potential of the N_2 molecule (9.8 eV), a large fraction of nitrogen is in molecular form. Indeed, molecular bands of N_2 are commonly seen in Perseid spectra (Cook *et al.*, 1971; Borovička and Boček, 1995). O_2 has much lower dissociation potential (5.1 eV) but the absence of O_2 bands is not conclusive because no strong bands of O_2 exist in the appropriate spectral region. In any case, it would be better to determine the N and O abundances from the strong infrared lines. Published IR spectra have, however, not been calibrated. The estimate for the TVS 29 spectrum (Borovička and Boček, 1995) gives $N/O \approx 2.5$, showing that the problem may be less severe in this case.

Luminous efficiency

The luminous efficiency, τ , expresses which part of the kinetic energy lost by a meteoroid ablating in the atmosphere is being converted into radiation. It is found in the classical luminosity equation :

$$I = -\tau \frac{v^2}{2} \frac{dm}{dt} \quad (1)$$

where I is the meteor's luminosity, v its velocity, m its mass and t time. By integrating equation (1), the unknown meteoroid initial mass, m_∞ , can be determined from the known luminosity and velocity as a function of time. For this purpose, luminosity is usually expressed in magnitude based units

$$I = 10^{-0.4M} \quad (2)$$

where M is the absolute (100 km distance) meteor magnitude. Velocity is given in cm s^{-1} and mass in grams. The mass determined this way is called *photometric* mass. For fast cometary meteors it is the only possibility to determine meteoroid mass because the *dynamic* mass cannot be derived owing to negligible deceleration.

The luminous efficiency is, however, a poorly known quantity. It depends on velocity. For velocities larger than

27 km s^{-1} , the formula of Ceplecha and McCrosky (1976) is usually used :

$$\log \tau = -13.69 + \log v \quad (3)$$

where v is given in km s^{-1} . This gives $\log \tau = -11.9$ for Perseids ($v = 60 \text{ km s}^{-1}$). We will try to determine the luminous efficiency independently from the Perseid spectra analyzed in the present paper.

To estimate the mass loss rate, we use the ratio of the instantaneous mass of the meteoritic part of the radiating gas to the relaxation time (i.e. the time spent by the ablated atoms in the radiating gas) :

$$\frac{dm}{dt} \approx \frac{m_G}{t_R}. \quad (4)$$

The relaxation time can be estimated from a meteor flare as the interval between the flare onset and the beginning of the decline (Fig. 5). For the flare at 79.5 km in spectrum A $t_R \approx 0.011 \text{ s}$ was found. The mass of the radiating gas can be determined from the total number of iron atoms, N_{Fe} , as given in Table 2 :

$$m_G = \frac{N_{\text{Fe}} A_{\text{Fe}}}{f_{\text{Fe}}} \quad (5)$$

where $A_{\text{Fe}} = 9.3 \times 10^{-23} \text{ g}$ is the mass of iron atom and f_{Fe} is the mass fraction of iron in the meteoroid. We assume $f_{\text{Fe}} = 18.5\%$ as in carbonaceous chondrites (Anders and Grevesse, 1989).

Even though some doubts can be raised on the correctness of the estimation of dm/dt , the most problematic quantity is, paradoxically, the meteor magnitude M . Unlike slow and bright meteors, where numerous optically thick lines are present and the spectrum approaches a black body spectrum (Borovička, 1993; Borovička and Spurný, 1996), the luminosity of bright Perseids and other fast meteors is governed by several bright lines. The observed magnitude then strongly depends on the spectral window used and on the sensitivity of the detector as a function of wavelength. In particular, it is important whether the radiation of H and K lines and of the infrared oxygen lines is included in the magnitude determination.

Knowing the meteor spectrum, the V magnitude in the international UBV photometric system can be computed from the formula (Allen, 1973) :

$$V = -2.5 \log \left(\int_0^{\infty} V_\lambda F_\lambda d\lambda \right) - 13.74. \quad (6)$$

The spectral flux F_λ in $\text{erg cm}^{-2} \text{s}^{-1} \text{\AA}^{-1}$ is related to the intensity I_λ given in Fig. 3 by $F_\lambda = I_\lambda / R^2$, where $R = 100 \text{ km}$. V_λ is the V filter passband; it is greater than 0.1 between 4900 and 6400 \AA . The emissions in blue and violet, including the H and K lines, do not influence the V magnitude. In fact no strong lines of the second component contribute to the V magnitude.

The V magnitude was used to compute V-band luminous efficiency τ_v . The resulting values are given in Table 4 together with the V magnitudes. The average luminous efficiency is close to $\log \tau_v = -11.9$ for both meteors. However, a systematic trend is present, the efficiencies being larger in the middle of the meteor bright part. At

Table 4. V-Band luminous efficiencies of two Perseid meteors

Point No.	Spectrum A		Spectrum B	
	V	$\log \tau_v$	V	$\log \tau_p$
1	-10.10	-12.0	-9.40	-12.1
2	-10.71	-12.0	-10.12	-11.9
3	-9.54	-11.8	-10.19	-11.9
4	-10.27	-11.7	-9.56	-11.8
5	-9.88	-11.9	-9.30	-11.9
6	-10.54	-11.9		
7	-9.85	-11.9		
8	-9.32	-12.0		
Average		-11.89		-11.93

first sight it seems that this could be correlated with the strength of the second component. A more detailed evaluation, however, showed that the role of the second component in the variation of τ_v is negligible. The situation is more complicated. Let us, for example, consider the fact that for a given mass of the radiating gas, higher temperature leads to higher intensity of spectral lines and hence to higher luminous efficiency. However, higher temperature also leads to higher ionization which causes a decrease of luminosity because the ions of such elements as Fe, Mg, Na have much fainter lines in the visual region than neutral atoms of the same elements. So, various effects acting in different directions are present even for the main component.

Our resulting average luminous efficiency is in surprisingly good agreement with the value of Ceplecha and McCrosky (1976). However, their value refers to meteor magnitude defined in a different way. In fact, V magnitude cannot be determined from normal non-spectral photographic meteor observation. Instead, the panchromatic magnitude, M_p , is used to express meteor brightness and to compute photometric mass. Ceplecha (1987) gave the following formula for panchromatic magnitude of stars of normal spectral types:

$$M_p = V + 0.62(B - V) - 0.52(V - R). \quad (7)$$

Meteor panchromatic magnitude is determined by measuring and comparing the images of meteor and stars. The emissions in the 3500–6600 Å range contribute to meteor panchromatic magnitude.

We did not use spectral photographs to determine panchromatic magnitude because they are influenced by the presence of spectral grating. Instead, we took the results of classical photometry of meteor DMS-89046 (spectrum B) performed by van Oudheusden and van Dijk (1991). They used short focal length cameras with rotating shutters and gave the magnitude for individual shutter breaks separated by 0.04 s, corresponding to about 2 km in height. This is a much lower resolution than we reached (Fig. 4), but we can compare their maximal magnitude at the height of 79 km ($M_p = -11.5$) with our value in this region (points 2 and 3, $V = -10.1$). This gives the “color index” $M_p - V = -1.4$ and, correspondingly, the panchromatic luminous efficiency $\log \tau_p = \log \tau_v + 0.56 \approx -11.4$. The higher panchromatic efficiency is clearly caused by the presence of the Ca II lines and other bright emissions in blue and violet.

In summary, we recommend to use the panchromatic luminous efficiency of $\log \tau_p = -11.4$ for Perseids (and other meteors with similar velocity) of brightness about -10 mag. Faint Perseids have probably different luminous efficiency owing to the lower relative brightness of the meteoritic lines in the second spectral components and larger role of the N₂ bands. In any case, the luminous efficiency of fast meteors strongly depends on the photometric band used.

Our panchromatic value is about three times higher than that used previously (Ceplecha and McCrosky, 1976). Ceplecha (1996), analyzing the Lost City meteorite fall, found the luminous efficiency for velocity of 13 km s⁻¹, ten times higher than previously used ($\log \tau_p = -11.4$ versus -12.4). This was explained by the dependence of luminous efficiency on meteoroid mass, the higher value being valid for bodies in the 10 kg range, the lower for 10 g bodies. Our results indicate that the scale is to be adjusted also at high velocities, although the mass of the meteoroids studied here is not particularly large. Using the above derived gas masses m_G and relaxation time t_R , the initial mass of the meteoroid DMS-85016 was estimated to 80 g and of DMS-89046 to 40 g.

Using the known spectrum, we can also compute the total radiative output of the meteor in all directions between two wavelengths, λ_1 and λ_2

$$L_{\lambda_1, \lambda_2} = 4\pi \int_{\lambda_1}^{\lambda_2} I_\lambda d\lambda. \quad (8)$$

L is obtained in erg s⁻¹ and can be directly compared with the kinetic energy loss rate computed as above. For example, at point 6 in spectrum A, the loss of kinetic energy is 3×10^{16} erg s⁻¹. It was found that 2.4% of this value is radiated out between 3500 and 6600 Å. A total of 1.4% is due to the Ca II H and K lines, 0.6% by the radiation above 4000 Å and 0.4% by the radiation below 3900 Å. These data are not particularly certain owing to the uncertain calibration of Ca II lines, but the large role of the radiation in the violet part of the spectrum is obvious.

Conclusions

We have observed and analyzed two spectra of bright Perseids. Three main aspects have been studied—the relation of two spectral components, chemical composition of the meteoroids, and meteor luminous efficiency. In addition, a qualitative explanation of the Russel (1960) effect in meteor flares was presented.

Two spectral components were identified in agreement with previous findings (Borovička, 1994). The temperature of the main component changed in the range 4400–4800 K, the second component is consistent with the temperature of 10,000 K. The mass of the radiating gas fluctuated, causing the fluctuation of the meteor brightness. The ratio of the second component to the main component gas varied as well, though more smoothly: from about 1:100 at the beginning to 1:15 in the middle and 1:30 at the end of the bright part of the meteors. This ratio proved to be not an unambiguous function of meteor velocity, height and brightness; it depends on the previous evolution of ablation. The most probable interpretation

is that the enhancement of the second component is a consequence of the development of a strong ablation shock wave. On the other hand, infrared meteor observation show that atmospheric lines behave differently and that a $\approx 10,000$ K air is present also at the beginning. More theoretical studies are needed to clarify these observational evidences.

In contrast to slower meteors, ablated calcium was completely evaporated in the observed Perseids. Within the observational error, i.e. within a factor of two, the elemental ratios of Fe, Na, Mg, Si, Ca, Cr, and Mn were found consistent with the abundances in carbonaceous chondrites and comet Halley. This is not surprising for cometary meteoroids. The same conclusion was made for Fe, Na, Mg, and Ca in Giacobinid meteors by Millman (1972) on the basis of a quite different method. More interestingly, the hydrogen content proved significantly lower than in comet Halley dust and probably lower than in carbonaceous chondrites. This can be explained by a loss of volatiles when the meteoroids approached the Sun to 0.9 AU at perihelion.

The V-band luminous efficiency was found to vary in the range $\log \tau_v = -11.8$ to -12.0 in magnitude based/c.g.s. units. The panchromatic luminous efficiency is higher owing to the presence of bright lines of Ca II in the violet. We recommend to use the value of -11.4 for very bright Perseids. This value is three times higher than that used up to now. It was estimated that about 1.5% of meteoroid kinetic energy was radiated out in the Ca II lines and 1% in all other lines between 3500 and 6600 Å.

Acknowledgements. We acknowledge the use of the electronic form of the table from Sviderskiene (1988) at CDS, Strasbourg. The first author was supported by grant No. 303406 from the Academy of Sciences of the Czech Republic and by grant No. 1862 from the Grant Agency of the Czech Republic.

References

- Allen, C. W. (1973) *Astrophysical Quantities*. Althone Press, London.
- Anders, E. and Grevesse, N. (1989) Abundances of the elements: meteoritic and solar. *Geochim. Cosmochim. Acta* **53**, 197–214.
- Betlem, H. and de Lignie, M. (1985) Twee vuurboltrajekten. *Radiant, J. Dutch Met. Soc.* **7**, 126–128.
- Borovička, J. (1993) A fireball spectrum analysis. *Astron. Astrophys.* **279**, 627–645.
- Borovička, J. (1994) Two components in meteor spectra. *Planet. Space Sci.* **42**, 145–150.
- Borovička, J. and Boček, J. (1995) Television spectra of meteors. *Earth, Moon, and Planets* **71**, 237–244.
- Borovička, J. and Spurný, P. (1996) Radiation study of two very bright terrestrial bolides and an application to the comet S-L 9 collision with Jupiter. *Icarus* **121**, 484–510.
- Ceplecha, Z. (1964) Study of a bright meteor flare by means of emission curve of growth. *Bull. Astron. Inst. Czechosl.* **15**, 102–112.
- Ceplecha, Z. (1987) Geometric, dynamic, orbital and photometric data on meteoroids from photographic fireball networks. *Bull. Astron. Inst. Czechosl.* **38**, 222–234.
- Ceplecha, Z. (1996) Luminous efficiency based on photographic observations of Lost City fireball and implications to the influx of interplanetary bodies onto Earth. *Astron. Astrophys.* **311**, 329–332.
- Ceplecha, Z. and McCrosky, R. E. (1976) Fireball end heights: a diagnostic for the structure of meteoritic material. *J. Geophys. Res.* **81**, 6257–6275.
- Cook, A. F., Halliday, I. and Millman, P. M. (1971) Photometric analysis of spectrograms of two Perseid meteors. *Can. J. Phys.* **49**, 1738–1749.
- Halliday, I. (1961) A study of spectral line identifications in Perseid meteor spectra. *Publ. Dominion Obs. Ottawa* **25**(1), 3–16.
- Halliday, I. (1969) A study of ultraviolet meteor spectra. *Publ. Dominion Obs. Ottawa* **25**(12), 315–322.
- Halliday, I. (1987) The spectra of meteors from Halley's comet. *Astron. Astrophys.* **187**, 921–924.
- Harvey, G. A. (1973a) Spectral analysis of four meteors. In *Evolutionary and Physical Properties of Meteoroids*, eds C. L. Hemenway, P. M. Millman and A. F. Cook, NASA-SP 319, pp. 103–129.
- Harvey, G. A. (1973b) Elemental abundance determinations for meteors by spectroscopy. *J. Geophys. Res.* **78**, 3913–3926.
- Jessberger, E. K., Christoforidis, A. and Kissel, J. (1988) Aspects of the major element composition of Halley's dust. *Nature* **322**, 691–695.
- Kokchirova, G. I. (1993) The quantitative analysis of the Perseid meteor spectra. *Astron. Vestnik* **27**(3), 100–112.
- Millman, P. M. (1972) Giacobinid meteor spectra. *J. R. Astron. Soc. Canada* **66**, 201–211.
- Millman, P. M. and Halliday, I. (1961) The near-infra-red spectrum of meteors. *Planet. Space Sci.* **5**, 137–140.
- Millman, P. M., Cook, A. F. and Hemenway, C. L. (1971) Spectroscopy of Perseid meteors with an image orthicon. *Can. J. Phys.* **49**, 1365–1373.
- Russel, J. A. (1960) A time resolved spectrum of the terminal burst of a Perseid meteor. *Astrophys. J.* **131**, 34–37.
- Sviderskiene, Z. (1988) Mean energy distributions in the stellar spectra of different spectral types and luminosities. I. Normal stars. *Bull. Vilnius Obs.* **80**, 7–104.
- van Oudheusden, J. P. and van Dijk, M. (1991) Astrometrisch en fotometrisch onderzoek aan de vuurbol van 13 augustus 1989, 2^h27^m40^s UT. *Radiant, J. Dutch Met. Soc.* **13**, 36–41.